Published in final edited form as:
Nano Lett. 2005 October ; 5(10): 1883–1888.

Stretching DNA using the Electric Field in a Synthetic Nanopore

Jiunn B. Heng[†], **Aleksei Aksimentiev**[†], **Chuen Ho**[†], **Patrick Marks**[†], **Yelena V. Grinkova**[‡], **Steve Sligar**[‡], **Klaus Schulten**[†], and **Gregory Timp**[*,†]
Beckman Institute, University of Illinois, Urbana, IL USA

Abstract

The mechanical properties of *DNA* over segments comparable to the size of a protein-binding site (3–10nm) are examined using an electric field-induced translocation of single molecules through a nanometer diameter pore. *DNA*, immersed in an electrolyte, is forced through synthetic pores ranging from 0.5 to 1.5nm in radius in a 10nm thick Si_3N_4 membrane using an electric field. To account for the stretching and bending, we use molecular dynamics to simulate the translocation. We have found a threshold for translocation that depends on both the dimensions of the pore and the applied transmembrane bias. The voltage threshold coincides precisely with the stretching transition that occurs in dsDNA near 60pN.

Keywords

Synthetic nanopore; Single molecule detection; DNA stretching transition

The encyclopedic information encoded in the genome is packaged, copied, and transcribed through protein mechanisms that exploit the distinctive physical properties of *DNA*. Recently, single molecule spectroscopies have been developed to infer the average elastic properties of long (48kbp~16.3μm) molecules from force-extension measurements. Bustamente et al.[1,2] have successfully fit this data over a range of forces (from *10fN* to *100pN*) using a simple worm-like chain model with the link length and extension modulus as parameters. When subjected to a force *>10pN*, *DNA* deforms, stretching the double helix. It is remarkable that near *60pN* a dramatic transition occurs—the double helix stretches from 107% to nearly 170% of the length of *B-DNA* over a few picoNewtons.[3,4] The distance between bases in the stretched *DNA* is 0.7nm; over 200% of the normal length.

Despite the success of this model, to capture the microscopic physics required to understand *DNA*-protein interactions, measurements of the mechanical properties of *DNA* over segments comparable to the size of a protein-binding site, which is about 10–30 base-pairs(bp) long (3–10nm), are required. We propose to test the elastic properties of *DNA* on this length scale by using the field-induced translocation of *DNA* across a membrane through a nanopore. [5–8] When an electric field is applied across the membrane with a pore in it, *DNA* immersed in electrolyte is attracted to the pore, blocks the current through it, and eventually permeates the membrane through the pore.[5–8] The forces acting on single nucleotides in a *DNA* strand during the translocation are approximately $F \sim qZ\Delta V/a$, where qZ is the effective charge per nucleotide, and ΔV is the electrostatic potential drop over the nucleotide separation a. Assuming, that $Z \approx 1$ and $a=0.34nm$, the force corresponding to the applied voltage can range from $0<F<1nN$. As a result of this force, it has already been shown that folds and bends can occur in *DNA* during

*gtimp@ebbtide.micro.uiuc.edu.
†Beckman Institute
‡Department of Biochemistry.

translocation through a 10nm diameter pore, which affects the current and the translocation kinetics.[9]

In this letter, we report the results of a stringent test of the nanometer-scale mechanical properties of *single DNA* molecules. Single molecules of double-stranded *DNA* (*dsDNA*) and single-stranded *DNA* (*ssDNA*), immersed in electrolyte, were forced through synthetic nanopores, ranging from 0.5 to 1.5nm in radius, in a 10nm thick Si_3N_4 membrane using an electric field. Molecular dynamics (MD) simulations provide a comprehensive account of the bending and stretching that accompanies a translocation. MD has identified a threshold for permeation of *dsDNA* through the pore that depends on the radius and the field. These predictions have been confirmed experimentally. The stretching transition that occurs near 60pN tension was found to determine the voltage threshold.

We formed membranes using conventional semiconductor fabrication practices described elsewhere.[10] Subsequently, a single nanopore is created in the membrane by electron beam stimulated decomposition and sputtering using a JEOL 2010F transmission electron microscope (TEM) operating at 200keV. Fig. 1(a) represents an array of TEM images taken at a tilt angle of 0° of pores with apparent radii of 0.5 ± 0.1nm, 0.95 ± 0.1nm and 1.5 ± 0.1nm in a Si_3N_4 membrane nominally 10nm thick. (To account for elliptical shape, the radius R_p is taken to be the geometric mean of the major and minor axis of the pore.) The thickness of similarly processed membranes was determined to be 10±2nm using scanning electron microscopy and 11±3nm using electron energy loss spectroscopy. The TEM images represent a two-dimensional projection through the membrane. The shot noise observed in the central area identified with the pore indicates perfect transmission of electrons through the membrane in that area. To investigate the three-dimensional structure, we tilted the membrane in the TEM about the pore axis and explored various defocus conditions. A model of the pore geometry that is consistent with this data is shown in Ho et al.[10], and Heng et al.[11] - two intersecting cones with a 10° cone angle - is represented schematically in the inset in Fig. 1(d).

To characterize molecular transport, we measured the electrolytic current through a pore as a function of the applied electrochemical potential at 23.5±1°C. The currents were measured using an Axopatch 200B amplifier in resistive feedback mode with a 100kHz bandwidth. All experiments were carried out in a membrane transport bi-cell made of either acrylic or PDMS, where the membrane separates two identical compartments each containing ≈ 40μL-1mL of 1M *KCl* electrolyte and a Ag/AgCl electrode. Fig. 1(d) shows the current-voltage (I-V) characteristics of the pores shown in Figs. 1(a–c), measured over a range of ±1V in 1M *KCl* after > 55 hours of immersion in de-ionized water. In all cases the I-Vs are approximately linear. A line fit to the data yields the conductance 0.63 ± 0.03nS, 1.09 ± 0.03nS and 1.24 ± 0.03nS. It is apparent that the conductance does not scale linearly with the radius derived from TEM. We attribute the observed variations in conductance to a fixed (negative) charge in the pore.[10]

Following the conductance measurements, *DNA* in 10mM *TRIS-Cl* buffer at pH 8.5 was injected at the negative electrode. A voltage was applied across the membrane and the current through the nanopore was measured. We have previously shown that under these conditions voltage-driven translocations of single molecules of *DNA* across the membrane temporary block the electrolytic current through the pore.[7] Using the pore as a stochastic sensor, we have also shown that the duration of the current transients can be used to discriminate between *ssDNA* and *dsDNA*, as well as *dsDNA* of various length.[7] Molecular dynamics simulations of *DNA* translocations through a synthetic nanopore[12] predict a translocation velocity of 400nucleotides/μsec for an electric field of 1.4V/5.2nm (much faster than that observed in proteinaceous pore like alpha-hemolysin which shows a velocity of 10nucleotides/μsec at a similar field.[13] The narrow bandwidth (100kHz) of the measurement apparatus used in these

experiments limits the observation to transients longer than 10–100 μseconds. And even if the transient can be measured, it cannot be used to unambiguously discriminate between a translocation of *DNA* across the membrane and a temporary occlusion of the pore without a subsequent translocation.[10] Therefore, to establish unequivocally that *DNA* permeates a pore and to count the number of copies, the minute amount of the *DNA* near the positive electrode was amplified using PCR and analyzed by gel electrophoresis or by quantitative PCR. This same methodology was used by Kasianowicz[5] to first establish the correspondence between the number of current transients through an alpha-hemolysin pore and the number of ssDNA molecules translocating through the pore.

We tested the permeability of *ssDNA*(58-mer) and *dsDNA*(58bp) through the pores shown in Figs. 1(a–c) using an applied voltage of 200mV across the membrane. Typical gel arrays are shown in Figs. 1(e,f,g) along with a molecular weight (MW) reference denoted as "100bp ladder," which contains a spread of *DNA* MW. After staining, the *DNA* in each lane can be seen as bands spread according to the length (or MW). Notice that the *ssDNA* collected at the positive electrode, denoted by (+)58-mer, is observed to permeate through all three pores and gives the same amplified pattern as the *ssDNA* injected at the negative electrode, denoted by (−)58-mer. On the other hand, *dsDNA* only permeates the R_p=1.5nm±0.1nm pore at 200mV.

We constructed a microscopic model of the experiment and carried out MD simulations of electrophoretic transport through pores. A crystalline Si_3N_4 membrane was built by replicating a unit cell of β-Si_3N_4 crystal along the unit cell vectors, producing a hexagonal patch of 10.3 nm thickness and 4.6 nm sides. By removing atoms from the Si_3N_4 patches we produced pores of symmetric double-conical (hourglass) shapes with radii that correspond to our experiments. A *DNA* double helix with the same sequence used in our experiments was built from individual base pairs in the geometry suggested by Quanta.[14] First, the *DNA* was placed in front of the pore, normal to the membrane, and then the Si_3N_4 DNA complex was solvated in pre-equilibrated TIP3P water molecules. K^+ and Cl^- ions were added corresponding to a 1M concentration. The final system measured about 30.3 nm in the direction normal to the membrane and included about 160,000 atoms. In order to simulate the system, the molecular force field describing water, ions and nucleic acids[14] was combined with the MSXX molecular force field for Si_3N_4.[15] The protocols are described elsewhere.[12]

At first, we simulated the 0.7nm-, 1.0nm- and 1.5nm-radii pores combined with one 58-bp *dsDNA* helix. To shorten the translocation times to a practical duration, the simulations were done at 1.3V. We applied a uniform electric field across a 10.3nm thick Si_3N_4 membrane to drive a 58bp dsDNA through 0.7nm- and 1.0nm-radius pores. The field induced a rearrangement of the ions and water that, in turn, focused the field to the vicinity of the membrane abolishing the gradient in the bulk, and producing a 1.3V transmembrane bias. Fig. 2(a) shows the position of the *dsDNA* center of mass (CoM) relative to the center of the Si_3N_4 membrane against time. Within the first few nanoseconds, the electric field drove *dsDNA* into the pores; the wider pore facilitated faster translocation. Due to their conical shapes, both pores narrow towards the center of the membrane, which slowed down *DNA* translocation. After about 4.5ns, the translocation halted in both simulations *before* the *DNA* arrived at the narrowest part of the pores. The snapshots included in the inset illustrate the conformations of *dsDNA* at the end of these simulations. Noticed that *dsDNA* traveled a longer path inside the wider pore suggesting that the translocation halts at a particular cross-section. To ascertain if the translocation halted at the same cross-section in both pores, we plot in the insert of Fig. 2 (a) the local diameter of the pore around the first *DNA* base pair. In both simulations, the translocation of *dsDNA* halted when the pore narrowed to 1.25±0.1nm-radius. So, we conclude that pores with R_p<1.25nm are impermeable to *dsDNA* for fields <1.3V/10nm, in agreement with the experiments.

To determine if a higher field could drive *dsDNA* through the same pores, we continued our simulations from the conformations shown in Fig. 2(a), applying a 6.5V transmembrane bias. In Fig. 2(b), we plot the position of the *dsDNA* CoM against the simulation time. The results of these simulations suggest that *dsDNA* can permeate both pores at a sufficiently high voltage. In the case of a 1.0nm-radius, the 6.5V bias deformed the *DNA* helix, shifting one of the strands relative to the other by approximately one nucleotide, while preserving the hydrogen bonds between strands. Such stretching and shifting reduces the effective diameter of a double helix, allowing it to pass through the constriction of the pore without unzipping. In the case of the 0.7nm pore, 6.5V unzipped *dsDNA* before it reached the narrowest part of the pore. After denaturing, one of the two strands passed through the 0.7nm constriction, while the other strand remained at the same place where the unzipping occurred. In contrast, we found that *dsDNA* permeates a 1.5nm-radius pore at 1.3 V. In Fig. 2(b), the *dsDNA* CoM is plotted against time. Within the first 5ns, the field drove *dsDNA* into the 1.5nm-radius pore with a speed comparable to that inside the 0.7nm-and 1.0nm- pores. In the 1.5nm pore simulation, however, the translocation of *DNA* did not halt before reaching the center of the membrane. Instead, after about 11ns, one end of the *DNA* helix passed through the 1.5nm constriction. Shortly following that, this end adhered to the surface of Si_3N_4 on the other side of the pore ($z<0$). Such surface adhesion of nucleosides has been described in depth in Aksimentiev et al.[12] and Yeh and Hummer[17]. Driven by the field, the rest of the *DNA* helix continued the move through the pore, deforming the double helix of *DNA* into a loop, as shown in Fig. 2(b). A translocation like this was reported earlier.[12]

To establish the threshold field and the force required to drive *dsDNA* through the pore, we restarted our simulation of the 1.0nm-radius pore from the conformation shown in the inset of Fig. 2(a). In Fig. 2(c) we plot the *dsDNA* center-of-mass against time for biases ranging from 1.3 to 6.5V. These results indicate that *dsDNA* permeates a 1.0nm-radius pore for voltages ≥3.2V. At 3.9V, the DNA strands unzipped when entering the pore, which resulted in transient slow down of the translocation. The predicted thresholds were tested experimentally using two pores with 1.0±0.1nm- and 1.1±0.1nm-radii. The gel array in Fig. 3(a) indicates that 58bp *dsDNA* can be forced through a 1nm-radius pore if the applied voltage is >2.75V. Notice that we only observe a fluorescent band in the lane corresponding to the positive electrode, (+) 58bp, for an applied bias of 3V. We obtained a similar result for a 1.1nm-radius pore, but the observed threshold voltage was lower: 58bp *dsDNA* permeates the pore for V> 2.25V.

We also measured the number of *DNA* copies translocating near threshold by quantitative real-time PCR. Two PCR primers were designed to amplify a 72bp region within a 622 base target sequence. A TaqMan® probe was designed, mapping to this 72bp target sequence and labeled with an FAM reporter dye at the 5′-end and with a TAMRA quencher dye at the 3′-end. During amplification, the primers and the probe hybridize to the target sequence. Subsequently, during polymerization, the 5′ exonuclease activity of the *DNA* polymerase cleaves the probe releasing the reporter dye and resulting in increased fluorescence, which is proportional to the amount of target. Figs. 3(b,c) represent the results of qPCR analyses showing the number of copies found to permeate through the 1.0nm and 1.1nm-radius pores as a function of the applied potential. In correspondence with the 2.75V threshold obtained from the gel array for 58bp, the 1.0nm pore exhibits a threshold voltage of 2.5V for 622bp *dsDNA*. Similarly, the 1.1nm-radius pore shows a threshold voltage of 2V. The 0.25V discrepancy observed between the gel array and qPCR data may be attributed to the difficulties associated with capturing and handling such a small number of *DNA* copies.

To elucidate the origin of the sharp voltage threshold for permeation of *dsDNA*, we used MD to examine the potential inside a 1.0nm-radius pore. The distribution corresponding to 2.6V is shown in Fig. 4(b). The potential drops abruptly near the constriction and the corresponding force increases rapidly near the pore center, as illustrated in Fig. 4(a). At 2.6V, we estimate

the average force acting on a nucleotide at the leading edge of the *DNA* at about 45pN, while above threshold at 3.2V this force exceeded 60pN, sufficient to stretch the helix and allow the molecule to pass.

Acknowledgements

We gratefully acknowledge frequent discussions with Jean-Pierre Leburton and Narayana Aluru in the Beckman Institute, and the use of the Center for Microanalysis of Materials supported by a U.S. Department of Energy grant (DEFG02-91-ER45439). We also would like to thank Dr. Susan Power of Cellular Molecular Technologies Inc for her help in conducting the qPCR experiments. This work was funded by grants from the National Science Foundation (0210843), the Air Force (FA9550-04-1-0214), and the National Institutes of Health (P41-RR05969); computer time was provided through a National Resources Allocation Committee grant (MCA93S028).

References

1. Bustamante C, Smith SB, Liphardt J, Smith D. Curr Opin Struc Biol 2000;10:279.
2. Bouchiat C, Wang MD, Allemand JF, Strick T, Block SM, Croquette V. Biophysical J 1999;76:409.
3. Cluzel-Schaumann H, Rief M, Tolksdorf C, Gaub HE. Biophysical J 2000;78:1997.
4. Smith SB, Cui Y, Bustamante C. Science 1996;271:795. [PubMed: 8628994]
5. Kasianowicz JJ, Brandin E, Branton D, Deamer DW. Proc Natl Acad Sci 1996;93:13770. [PubMed: 8943010]
6. Meller A, et al. Phys Rev Lett 2001;86:3435. [PubMed: 11327989]
7. Heng JB, Ho C, Kim T, Timp R, Aksimentiev A, Grinkova YV, Sligar S, Schulten K, Timp G. Biophysical J 2004;87:2905.
8. Akeson M, Branton D, Kasianowicz JJ, Brandin E, Deamer DW. Biophysical J 1999;77:3227.
9. Li J, Gersho M, Stein D, Brandin E, Aziz MJ, Golovchenko JA. Nature Materials 2003;2:611.
10. Ho C, Qiao R, Heng JB, Chatterjee A, Timp R, Aluru N, Timp G. PNAS.
11. Heng JB, Aksimentiev A, Ho C, Dimitrov V, Sorsch TW, Miner JF, Mansfield WM, Schulten K, Timp G. Bell Labs Technical Journal 2005;10accepted
12. Aksimentiev A, et al. Biophysical J 2004;87:2086.
13. Mathe J, Aksimentiev A, Nelson DR, Schulten K, Meller A. PNAS. accepted by PNAS
14. Polygen. Quanta Polygen Corporation. 1988
15. Cornell WD, Cieplak P, Bayly CI, Gould IR, Merz KM Jr, Ferguson DM, Spellmeyer DC, Fox T, Caldwell JW, Kollman PA. J Am Chem Soc 1995;117:5179.
16. Wendel JA, Goddard W. J Chem Phys 1992;97:5048.
17. Yeh I, Hummer G. PNAS 2004;101:12177. [PubMed: 15302940]

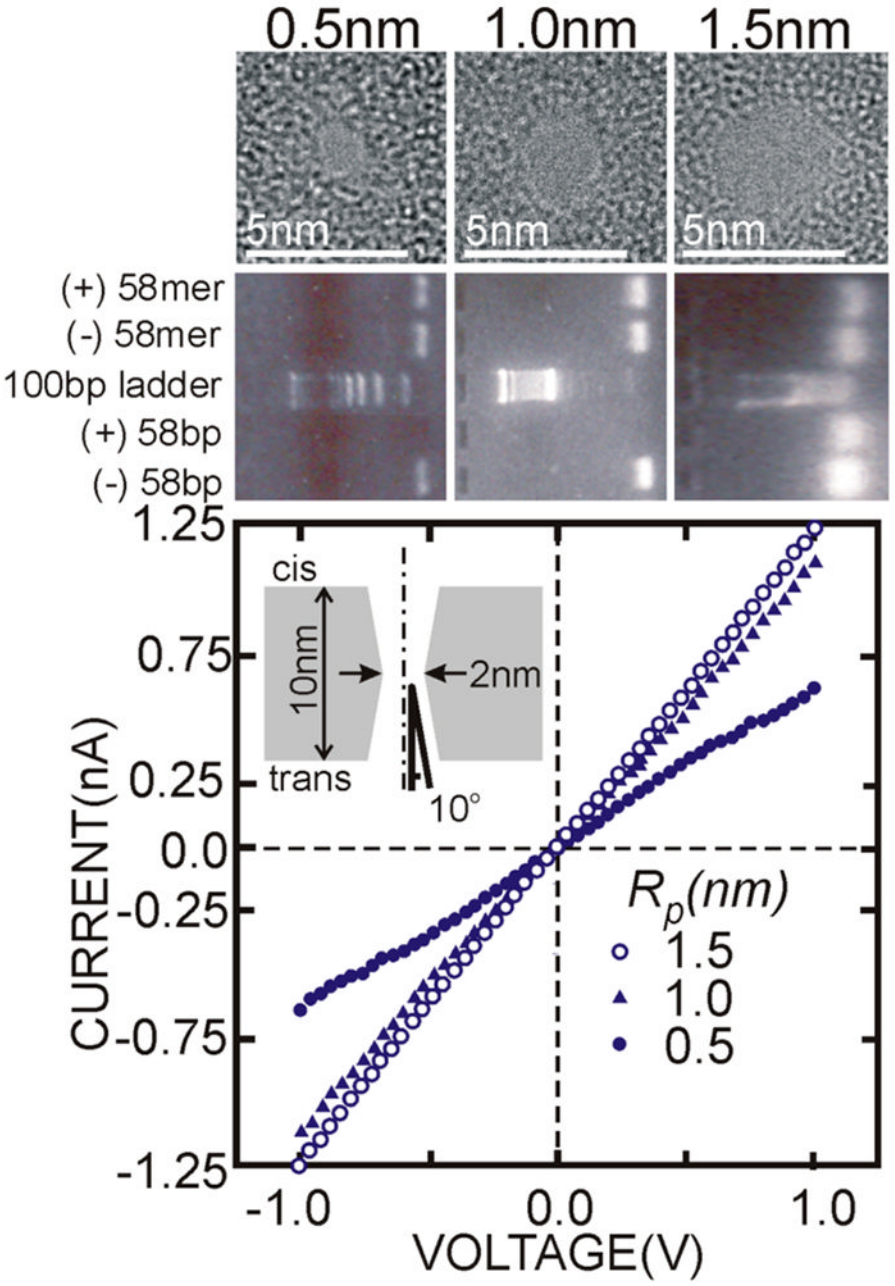

Figure 1.

(Top) TEM images of pores with apparent radii of 0.5 ± 0.1 (a), 0.95 ± 0.1 (b), and 1.5 ± 0.1 nm (c) in a 10 nm thick Si_3N_4 membrane at 0° tilt. ***(Middle)*** Gel arrays showing five horizontal lanes with fluorescent bands that identify 58-mer ss*DNA* and 58bp *dsDNA* at the positive (+) and negative (−) electrodes separated by 0.5nm (e), 1.0nm (f), and 1.5nm (g) pores (with 100bp ladder as a reference). The applied voltage was 200 mV. ***(Bottom)*** I-V characteristics in 1M *KCl* solution of the same three pores. Line fits yield slopes of 0.63 ± 0.03 nS, 1.09 ± 0.03 nS, and 1.24 ± 0.03 nS for the three pores, respectively.

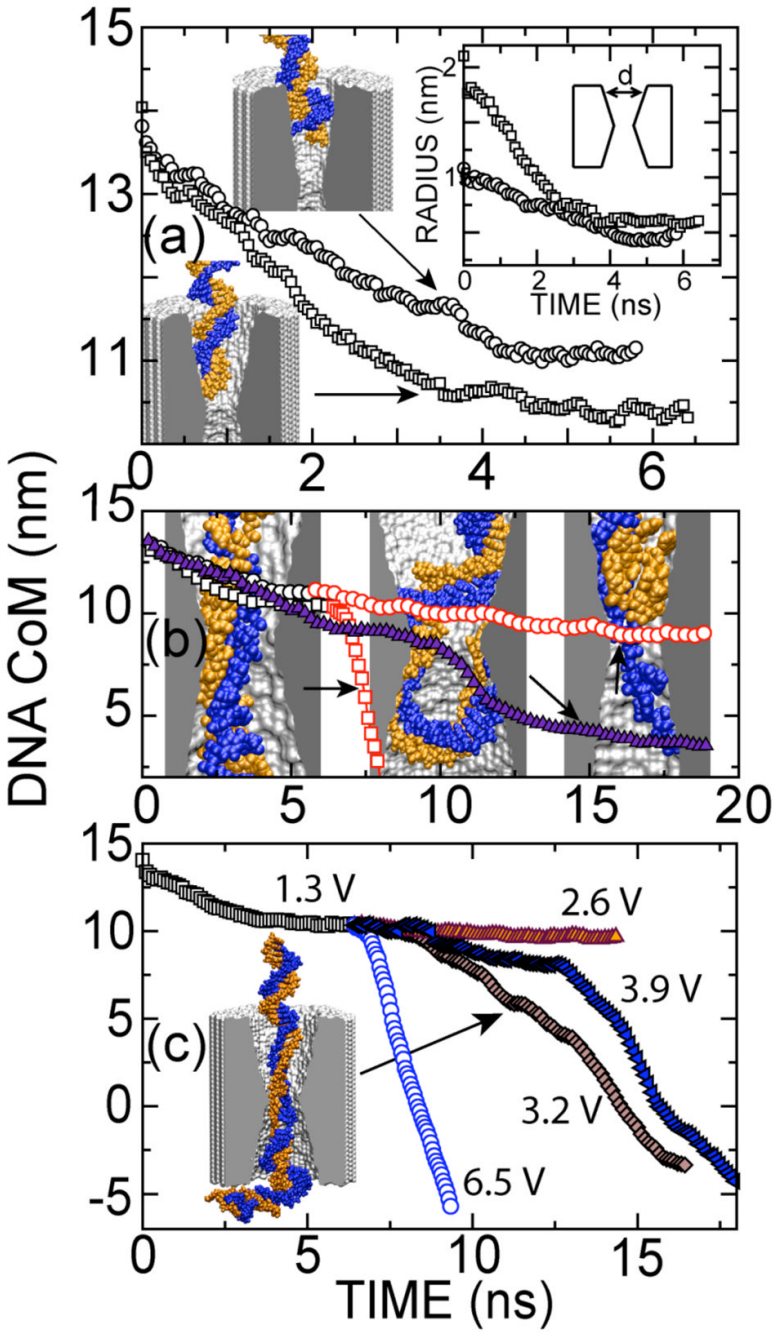

Figure 2.

(a) 1.3 V was applied to drive *dsDNA* into 0.7-nm-radius (circles) and 1.0-nm-radius (squares) pores. After about 4.5 ns, the translocation of *DNA* halted in both. The snapshots show the conformations of *DNA* at the end of these simulations. The inset to (a) shows the radius of the pore cross-section near the first base inside the 0.7nm and 1.0nm pores. The translocation of *dsDNA* halts when the pore narrows to 1.25±0.1nm. **(b)** Translocations of 58bp *dsDNA* through 0.7nm(circle), 1.0nm(square), and 1.5nm(triangle) radius pores. Black (1.3V) and red (6.5V) symbols reflect the applied bias. The snapshot on the left illustrates *dsDNA* permeating the 1.0-nm radius pore at 6.5V bias. This pore was not observed to conduct *dsDNA* at 1.3V bias. The middle snapshot shows the final conformation of *dsDNA* after passing through the narrowest

part of the 1.5nm radius pore at 1.3 V. The right illustrates the unzipping of the *dsDNA* inside the 0.7nm pore at 6.5 V. The snapshots are each of different scale. **(c)** *dsDNA* permeates a 1.0nm radius pore for voltages >3.2V. The snapshot illustrates the conformation of *dsDNA* at 3.2 V after 12ns.

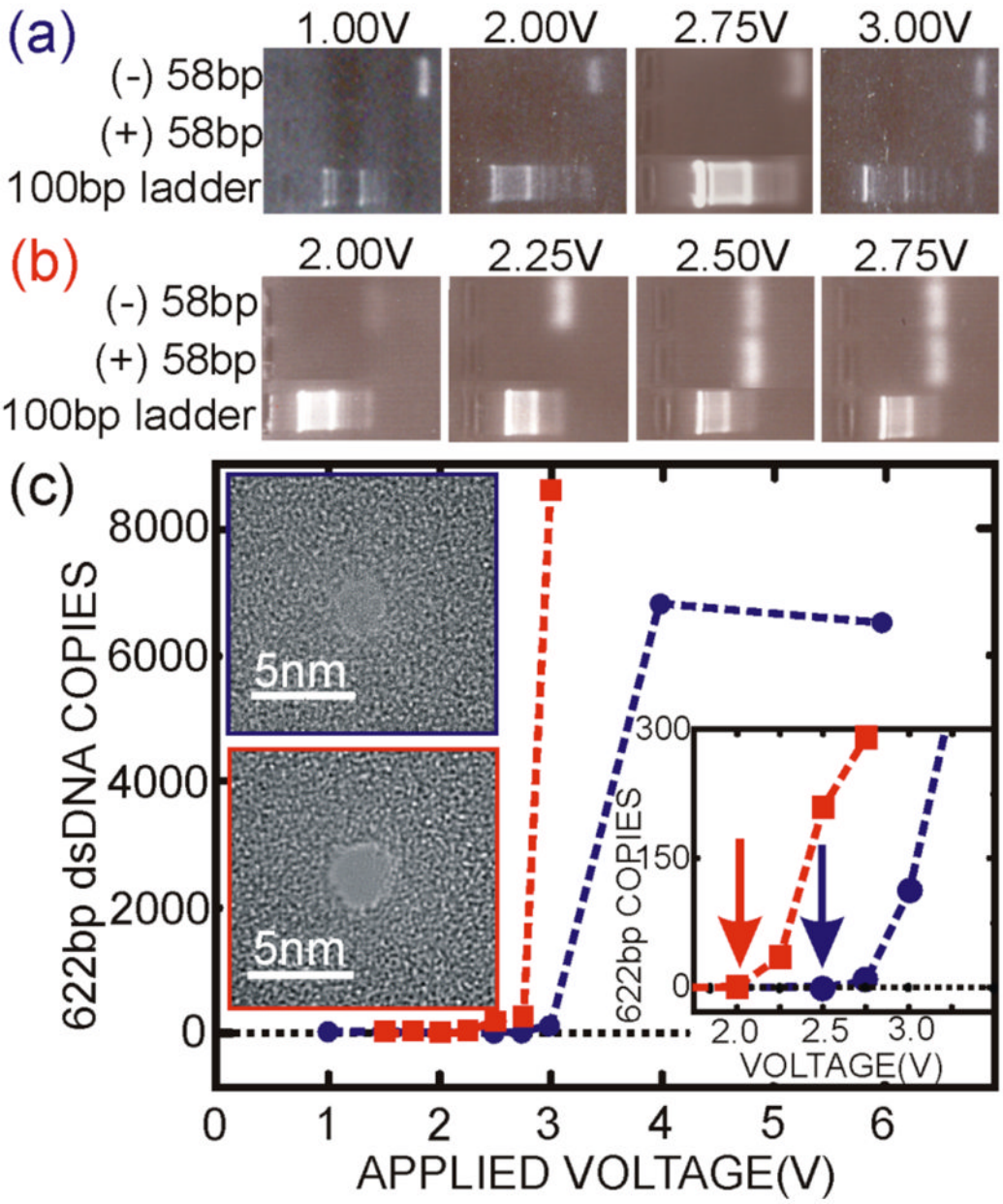

Figure 3.

(a) Gel arrays containing 3 horizontal lanes with fluorescent bands indicating 58bp *dsDNA* found at the negative (−) and positive (+) electrodes in a bi-cell with a 1nm radius pore (along with a 100bp ladder.) The 58bp permeates the pore only for V>2.75V. **(b)** Similar to (a) but instead using a 1.1nm radius pore. The 58bp permeates this pore only for V>2.25V. **(c)** qPCR results obtained for the same pores showing the copy number versus voltage. ***Upper left insets*** TEM micrograph taken at 0° tilt for 1nm radius (blue) and 1.1nm radius(red). 622bp *dsDNA* permeates the 1nm pore for V>2.5V, and the 1.1nm pore for V>2.25V. ***Lower right inset*** Expanded view of the data near threshold.

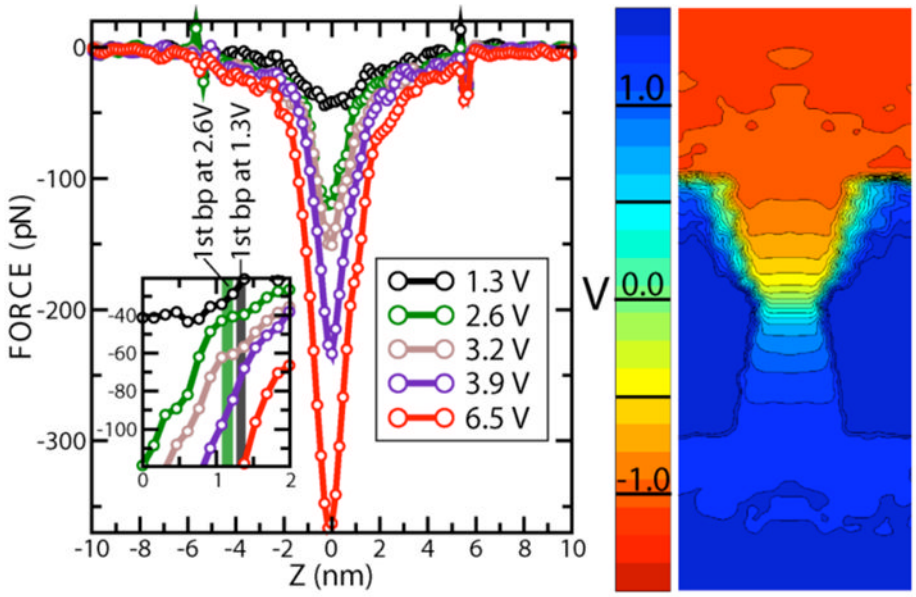

Figure 4.

(a) The force versus distance from the center of the pore. ***Inset*** Expanded view of the same data near threshold. The vertical bands indicated the location of the leading *DNA* base pair. **(b)** Electrostatic potential contours inside a 1.0nm-radius pore at 2.6 V.